NURETH14-234

BENCHMARK OF SIMULATE5 THERMAL HYDRAULICS AGAINST THE FRIGG AND NUPEC FULL BUNDLE TEST EXPERIMENTS

Gerardo Grandi¹ and Sten-Örjan Lindahl²

¹ Studsvik Scandpower, Inc, 504 Shoup Avenue, Suite 201, Idaho Falls, ID, U.S.A ² Studsvik Scandpower AB, Stensborgsgatan 4, SE-721 32 Västerås, Sweden

Abstract

SIMULATE5 is Studsvik Scandpower's next generation nodal code. The core portion of the thermal hydraulic models of PWR and BWRs are treated as essentially identical, with each assembly having an active channel and a number of parallel water channels. In addition, the BWR assembly may be divided into four radial sub-assemblies. For natural circulation reactors, the BWR thermal hydraulic model is capable of modeling an entire vessel loop: core, chimney, upper plenum, standpipes, steam separators, downcomer, recirculation pumps, and lower plenum. This paper presents results of the validation of the BWR thermal hydraulic model against: (1) pressure drop data measured in the Frigg and NUPEC test facilities; (2) void fraction distribution measured in the Frigg and NUPEC loops; (3) quarter-assembly void fraction measured in the NUPEC experiments and (4) natural and forced circulation flow measurements in the Frigg loop.

Introduction

SIMULATE5 (S5) is Studsvik Scandpower's next generation nodal code [1,2,3], which has been developed to address deficiencies of existing reactor physics tools for today's advanced core designs with increased heterogeneity and aggressive operating strategies. The core portion of the thermal hydraulic (TH) models of PWRs and BWRs are treated essentially identical, with each assembly having an active channel and a number of parallel water channels. In addition, the BWR assembly may be divided into four radial sub-assemblies to provide detailed feedback information to the neutronic model. For natural circulation reactors, S5's BWR thermal hydraulic model is capable of modeling an entire vessel loop: core, chimney, upper plenum, standpipes, steam separators, downcomer, recirculation pumps, and lower plenum.

Experiments in the Frigg loop with the OF64 test section [4] were designed as a full scale simulation of an 8x8 rod fuel assembly. Void fraction and two-phase pressure drop measurements include a wide range of operating conditions such as pressure, power, inlet subcooling and inlet throttling. The experimental results also include flow measurements under natural and forced circulation conditions. These measurements provide data to validate S5 natural and forced circulation capabilities.

The NUPEC experiments are the basis for the Full-size Fine-mesh Bundle Test Benchmark proposed by NEA/OECD in 2006 [5]. The NUPEC test program included void and pressure drop measurements using full size fuel bundles for BWRs. Radial void distribution

measurements at the end of the test sections were performed. Different axial and radial power shapes were considered. The radial void distribution measurements provide valuable information to partially validate S5's BWR quarter- assembly calculations.

1. SIMULATE5 thermal hydraulics

In S5, a BWR core is represented with one TH channel per fuel bundle. The assembly consists of a number of parallel flow channels (active coolant, water rod(s)), which are treated individually. In addition to the ordinary axial nodalization, (typically 25 nodes per channel), the conventional nodes are axially divided into sub-nodes such that each is materially homogeneous.

S5 TH [2] uses a four-equation model, vapour and liquid mass conservation, mixture energy conservation and mixture momentum conservation. The area-averaged form of the conservation equations employed by S5 is similar to the one appearing in the literature [6]. In addition to the conservation equations, closure relationships exits for each phasic density, defined as a function of the local pressure and phasic enthalpy. The general drift flux formulation for the void fraction completes the set of equations to be solved. The concentration parameter and the void-weighted drift velocity may be calculated from a library of void correlations. In this work, the EPRI correlation [7] has been chosen. The two-phase friction multiplier may be selected from a library of correlations also. The Martinelli-Nelson correlation has been selected for this work [6].

S5 offers a TH evaluation of each quarter-bundle as an option (below labelled Q-bundle) of a BWR assembly. First, the full assembly is analyzed in the "conventional" manner. Results from this analysis are used as boundary conditions (total assembly inlet flow, water rod flow conditions) to evaluate each quarter- bundle. For each type of assembly, the user specifies one of these alternatives to handle cross flow:

- Closed Q-assemblies (no cross flow): The Q-channel flow rates are adjusted until the total pressure drop of the sub-channels are identical. This option may be used for the SVEA fuel of Westinghouse.
- Open Q-assemblies: Cross flow driven by the lateral pressure difference. The lateral momentum equation is employed to compute cross flow, with turbulent mixing and void drift effects assumed to be negligible. At the bundle inlet, all four Q-channel flow rates are equal. This ad hoc assumption is justified by the fact that whatever incorrect inlet distribution exists will quickly disappear a few nodes up the assembly.

For natural circulation reactors, it is important to have a model which calculates the detail flow, pressure drop and void conditions in the core. Furthermore, an accurate prediction of the pressure drop and driving forces (elevation heads, friction and irreversible losses) in the recirculation loop is also required. S5 BWR TH is capable of modeling the entire vessel loop: core, chimney (for natural circulation reactors), upper plenum, standpipes, steam separators, steam dome, upper and lower down comer, recirculation pumps, and lower plenum. The same conservation equations as in the core are solved for each of the vessel components.

2. Frigg loop experiments

The OF64 test section was simulated using the S5 core channel mode. The balance of the experimental loop was simulated using the BWR vessel models available in S5. The next three subsections compare the S5 results against pressure drop measurements [8], void measurements [9] and natural and forced circulation flow measurements [10], respectively.

2.1 Pressure drop measurements

Simulations required only the test section model. Core exit pressure, inlet throttling, inlet subcooling, heating power in the rod cluster, and mass flux in the test section were boundary conditions for these calculations. The mass flux changes in the range from 500 to 2000 kg/m2/s, the heating powers range from 1978 to 5090 kW and the inlet subcooling is between 7 and 38 °C. The average pressure in the loop in this set of experiments is 6.8 MPa. Figure 1 compares the numerical and experimental results. The results show good agreement. The average bias is +1% and the standard deviation 3.6%.

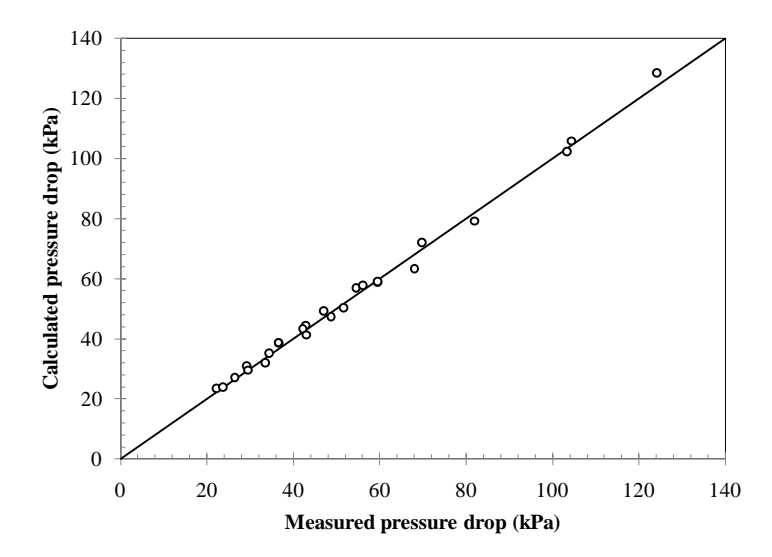


Figure 1 Frigg experiments. Comparison of two-phase pressure drop measurements.

Figure 2 shows the pressure drop distribution for two runs with similar power and flow conditions (power 3517 kW, mass flux 1253 kg/m2/s) but different subcooling, namely: run 704053 (inlet subcooling 7.5 °C) and run 704035 (inlet subcooling 22.4 °C).

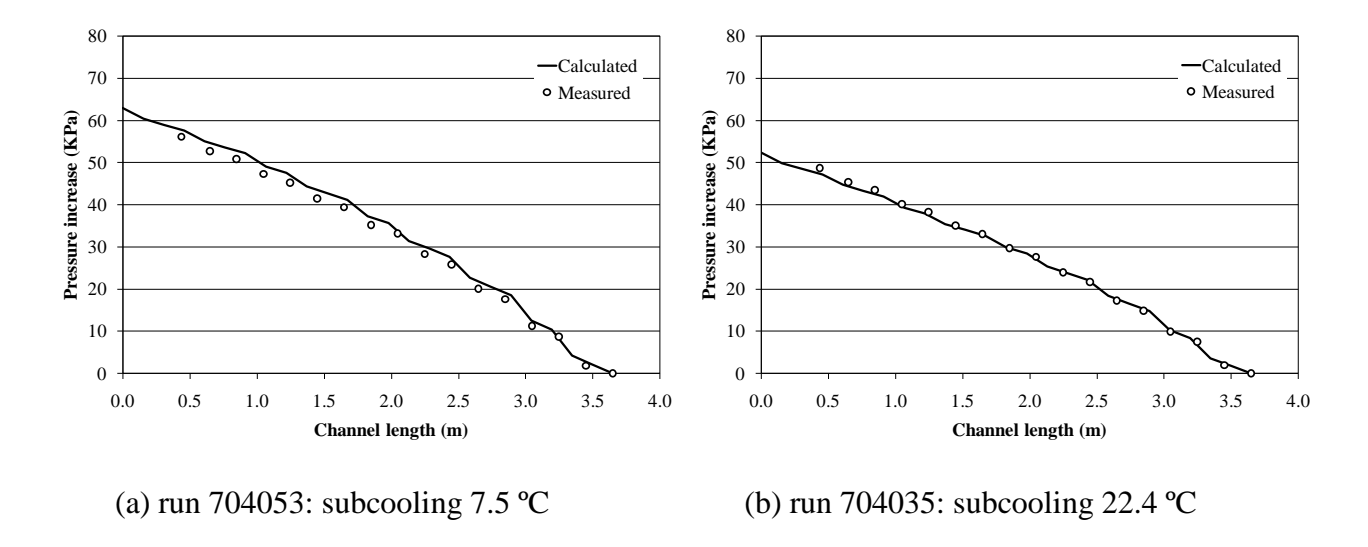


Figure 2 Axial pressure drop distribution for runs 704053 and 704035.

2.2 Void measurements

The boundary conditions applied in the simulations are the same as the ones applied in the simulation of the pressure drop measurements. The mass fluxes range from 500 to 2000 $kg/m^2/s$, the average heat fluxes range from 22.0 to 57.1 W/cm^2 and the inlet subcooling is between 9 and 38 °C. The results show good agreement with the measurements. The average bias is +0.2% and the standard deviation 2.3%.

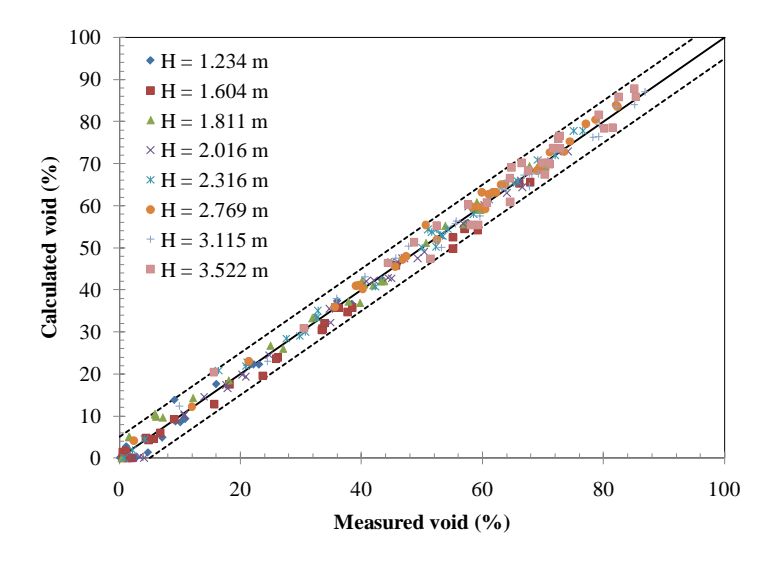


Figure 3 Frigg experiments. Comparison of void fraction measurements.

Figure 4 compares the void profiles for two runs with similar mass flux and heating power (mass flux 1258 kg/m2/s, power 3514 kW), but different inlet subcooling, namely: run 713021 (subcooling 24 °C) and run 713009 (subcooling 9.1 °C).

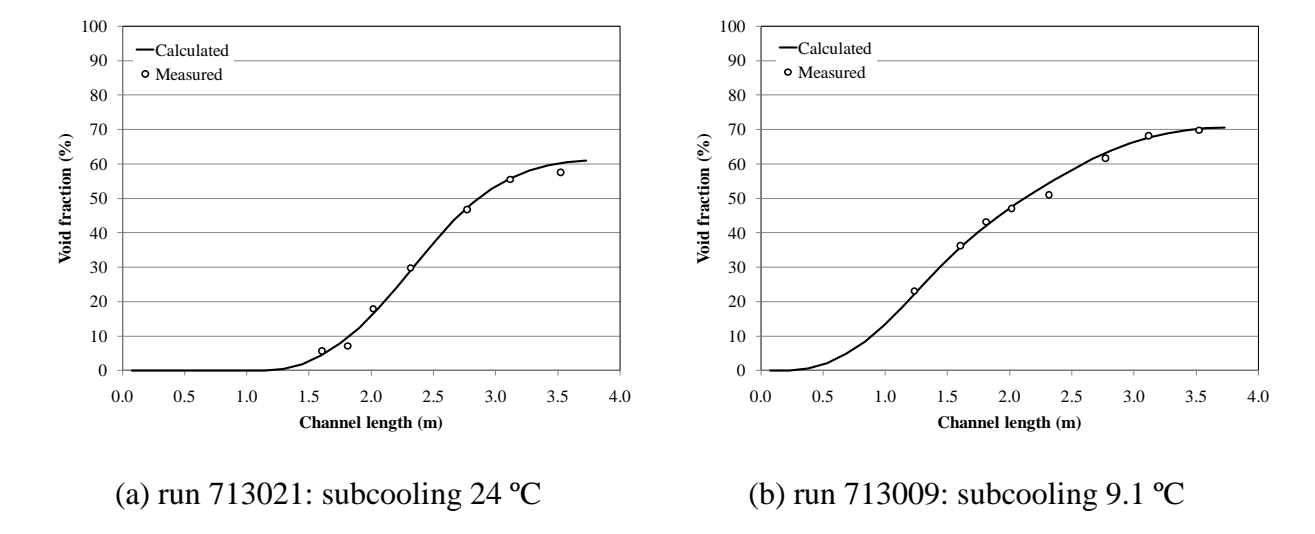


Figure 4 Axial void distribution for runs 713021 and 713009.

2.3 Steady state flow rates

The simulations were performed using the complete model for the experimental loop (i.e. both the test section and the recirculation loop were explicitly modelled). The heating power in the test section, the water level, the pump speed, the steam drum pressure, and the test section inlet subcooling were set as boundary conditions for the calculations. The total flow in the loop was calculated by S5.

Figure 5 shows the capability of S5 to compute the total core flow for the following experimental conditions: pressure 6.8 MPa, inlet subcooling 9 °C, inlet throttling 57 velocity heads, and pump speed 0 rpm, 500 rpm, 1000 rpm, and 1300 rpm. The lines represent the S5 solution and the points the experimental results. There is good agreement between the mass fluxes calculated by S5 and the measured ones. There is a tendency to over predict the mass flux at low heat flux at low pump speeds and natural circulation.

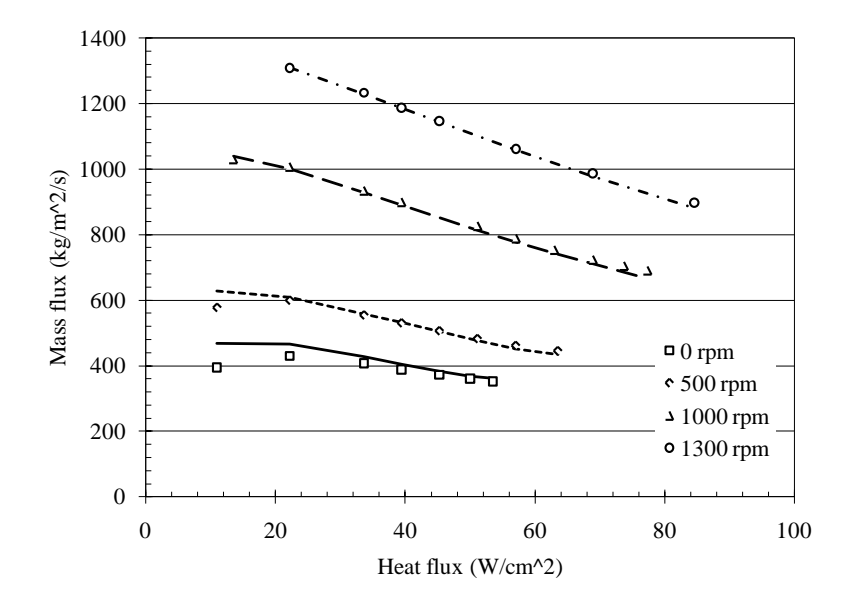


Figure 5 Frigg experiments. Steady state calculated mass flux as a function of heat flux.

3. BFBT benchmark

The BFBT test sections were simulated using the S5 core channel model. The test section exit pressure, inlet subcooling, heating power and inlet mass flow were boundary conditions for these calculations. The next subsections compare the S5 results against two-phase pressure drop measurements, cross-sectional void measurements and quarter-assembly void measurements.

3.1 Two-phase pressure drop measurements

A high burnup 8x8 BWR fuel assembly type with 60 heated rods was simulated. The axial power shape is cosine and the radial power shape resembles the pattern for beginning of operation (BOL). Experimental conditions are summarized in Table 1.

Table 1 BFBT experiments. Two-phase pressure drop measurement conditions for Assembly C2A.

ASSEMBLY C2A	
Pressure (MPa)	7.2
Flow rate (t/h)	20 45 55 70
Inlets subcooling (kJ/kg)	50.2
Exit quality (%)	7 10 15 20 25

Figure 6 compares the numerical and experimental results. The numerical results show good agreement with the experimental data. The average bias is +1.7% and the standard deviation 1.7%.

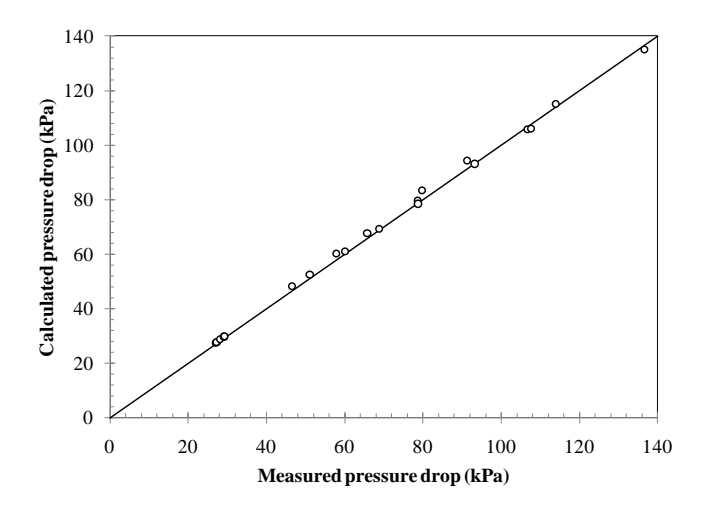


Figure 6 BFBT experiments. Comparison of two-phase pressure drop measurements.

3.2 Void measurements

A high burnup 8x8 BWR fuel assembly type with 60 heated rods was simulated. The axial power shape is uniform and the radial power shape resembles the pattern for beginning of operation. Experimental conditions for the selected cases are summarized in Table 2.

Table 2 BFT experiments. Void measurement conditions for Assembly 4.

ASSEMBLY 4	©©©©©©© ©©©©©©©© ©©©©©©©©©©©©©©©©©©©
Pressure (MPa)	7.2
Flow rate (t/h)	10, 20, 30, 45, 55, 70
Inlet subcooling (kJ/kg)	20.9, 50.2, 126
Exit quality (%)	2, 5, 8, 12, 18, 25

A total of 36 measurements were simulated. Figure 7 compares the numerical and experimental results. The numerical results show good agreement with the experimental data. The average bias is +0.9% and the standard deviation 1.9%.

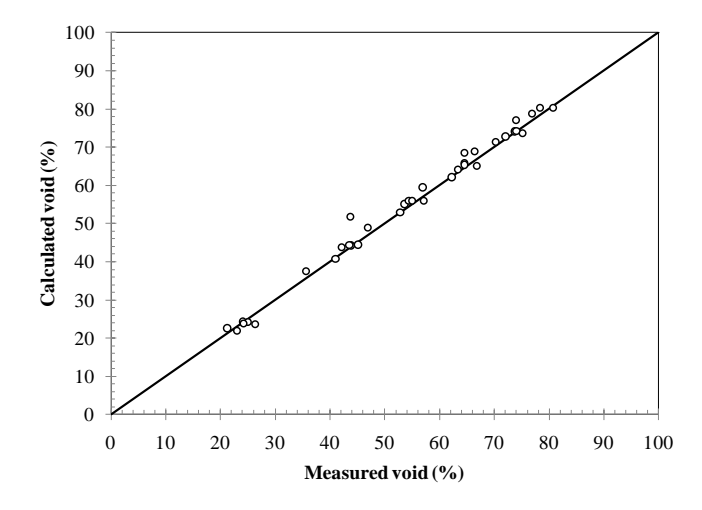


Figure 7 BFBT experiments. Comparison of Assembly 4 void measurements.

3.3 Effect of the radial and axial power shapes

A subset of the measurements for different assembly types with the same operating pressure (7.2 MPa) and test section inlet subcooling (50.2 kJ/kg) but different power, inlet flow, radial and axial power shapes was analyzed. A total of 15 measurements were simulated. Table 3 summarizes the operating conditions for these runs. Figure 8 and Table 4 summarize the results.

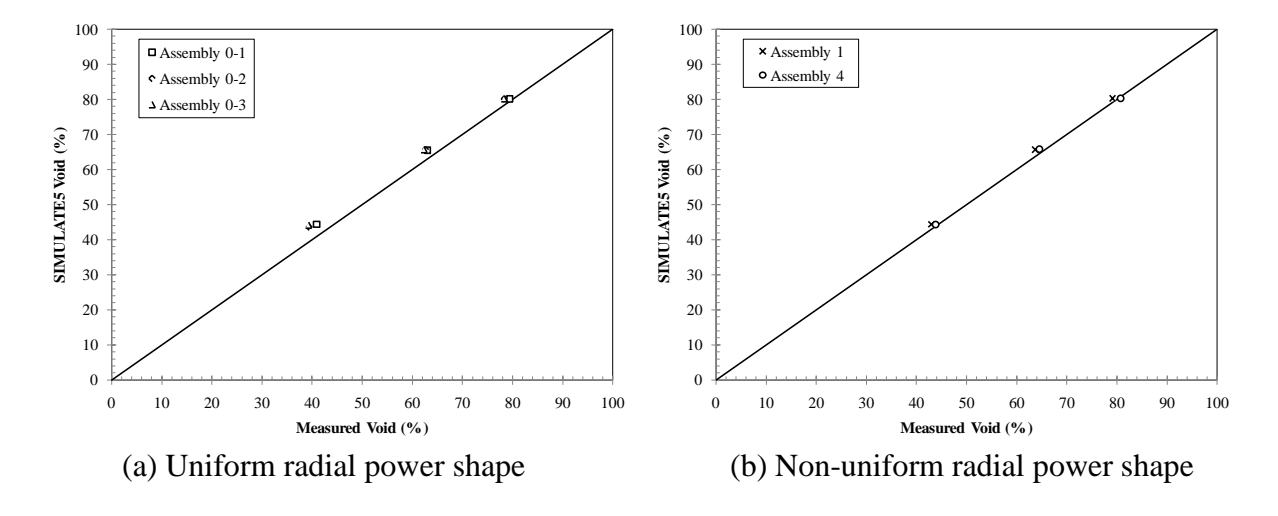


Figure 8 BFBT experiments. Effect of the radial and axial power shapes.

Table 3 Effect of the radial and axial power shapes. Selected runs, experimental conditions.

Assembly	Experiment	Heated	Radial	Axial	Flow	Power	Quality
	_			shape	(t/h)	(MW)	(%)
	0011-55		Uniform		54.03	1.90	5.0
0-1	0011-58	62		Uniform	54.90	3.51	12.0
	0011-61				54.79	6.44	25.0
	0021-16				54.85	1.91	5.0
0-2	0021-18	60	Uniform	Uniform	54.90	3.51	12.0
	0021-21				54.90	6.45	25.0
	0031-16	55	Uniform	Uniform	54.96	1.92	5.0
0-3	0031-18				54.79	3.52	12.0
	0031-21				54.90	6.45	25.0
	1071-55				54.61	1.92	5.0
1	1071-58	62	BOL	Cosine	55.07	3.52	12.0
	1071-61				54.65	6.48	25.0
4	4101-55		BOL	Uniform	54.59	1.92	5.0
	4101-58	60			54.58	3.52	12.0
	4101-61				54.65	6.48	25.0

Table 4 Effect of the radial and axial power shapes. Comparison of void measurements.

Assembly	Experiment	Exit quality (%)	Calculated exit quality (%)	Exit void (%)	Calculated exit void (%)	Difference exit void (%)
	0011-55	5.0	5.0	40.9	44.4	3.5
0-1	0011-58	12.0	12.0	63.0	65.5	2.5
	0011-61	25.0	25.0	79.4	80.1	0.7
	0021-16	5.0	4.8	39.4	43.5	4.1
0-2	0021-18	12.0	12.1	62.6	65.7	3.1
	0021-21	25.0	24.9	78.3	80.1	1.8
	0031-16	5.0	4.9	39.3	44.2	4.9
0-3	0031-18	12.0	12.1	62.3	65.7	3.4
	0031-21	25.0	25.0	78.3	80.2	1.9
	1071-55	5.0	4.9	43.0	44.4	1.4
1	1071-58	12.0	12.0	63.7	65.7	2.0
	1071-61	25.0	25.1	79.1	80.3	1.2
4	4101-55	5.0	4.9	43.8	44.3	0.5
	4101-58	12.0	12.1	64.5	65.8	1.3
	4101-61	25.0	25.1	80.7	80.3	-0.4

From Figure 8 and Table 4 the following observations can be made:

- For the same exit quality, the measured exit void depends on the axial and radial power shape.
- For the same exit quality, S5 calculated cross-sectional void fraction is independent of the axial and radial power distribution. This is to be expected for a 1D thermal hydraulic model.
- The bias in the exit void is a function of the exit quality. For a 5% exit quality the bias is +2.0% and reduces to $\sim +1.0\%$ for a 25% exit quality.
- The standard deviation is also a function of the exit quality. For a 5% exit quality the bias is 2.5% and reduces to 0.9% at 25% exit quality.
- S5 predictions are closer to the measurements for those assemblies with radial power distributions that resemble actual pin power distributions in a reactor, i.e. Assemblies 1 and 4.

3.4 Quarter- assembly void

Table 5 summarizes the operating conditions for the six runs selected for the quarter-assembly thermal hydraulic calculations. The calculations were performed using the open Q-assemblies option.

Assembly	Run	Heated Pins	Q- Assembly Power	Pressure (MPa)	Subcooling (kJ/kg)	Flow (t/h)	Power (MW)
	0011-55	0000000	1.02 0.07	7.180	52.6	54.03	1.90
	0011-58		1.03 0.97 0.97 1.03	7.172	51.0	54.90	3.51
	0011-61			7.210	50.9	54.79	6.44
	0031-16		1.09 1.02 1.02 0.87	7.180	52.4	54.96	1.92
0-3	0031-18	00000000 000@@@00 000@@@00		7.179	50.0	54.79	3.52
	0031-21	00000000		7.171	49.4	54.90	6.45

Table 5 Definition of the runs used in quarter-assembly calculations.

The cross-sectional void fractions at the test section outlet and the Q-assembly relative void fractions are compared against measurements in Table 6 and Table 7 for Assemblies 0-1 and 0-3 respectively.

Table 6 Quarter-assembly results Assembly 0-1.

Run 0011-	55 measure	d void (%)	SIMU	JLATE5 voi	d (%)	Di	fferences (%	(o)
Cross-sect	ional void	40.90	Cross-sectional void		44.57	Cross-sect	3.7	
Q-assembly	Q-assembly relative void			Q-assembly relative void			relative voi	d
y / x	1	2	y / x	1	2	y / x	1	2
1	1.00	1.01	1	1.04	0.96	1	3.2	-4.6
2	0.97	1.02	2	0.96	1.04	2	-1.0	1.7
Run 0011-	58 measure	d void (%)	SIMU	JLATE5 voi	d (%)	Di	fferences (%	6)
Cross-sect	ss-sectional void 63.00			tional void	65.62	Cross-sect	ional void	2.6
Q-assembly	assembly relative void			relative voi	id	Q-assembly	d	
y / x	1	2	y / x	1	2	y / x	1	2
1	1.01	1.01	1	1.02	0.98	1	0.8	-3.3
2	0.99	1.00	2	0.98	1.02	2	-0.7	2.2
Run 0011-	61 measure	d void (%)	SIMU	LATE5 voi	d (%)	Di	fferences (%	<u>(6)</u>
Cross-sect	sectional void 79.40		Cross-sectional void		80.22	Cross-sect	0.8	
Q-assembly	Q-assembly relative void		Q-assembly relative void Q-assemb			Q-assembly	relative voi	d
y / x	1	2	y / x	1	2	y / x	1	2
1	1.01	0.99	1	1.01	0.99	1	0.6	-0.5
2	1.01	1.00	2	0.99	1.01	2	-1.9	1.3

Table 7 Quarter-assembly results Assembly 0-3.

Run 0031-16 measured void (%)			SIMU	LATE5 voi	d (%)	Di	fferences (/ 6)
Cross-secti		39.30		ional void	44.38	Cross-sectional void		5.1
Q-asser	mbly relativ		Q-assembly relative vo		e void	Q-asse	e void	
y / x	1	2	y / x	1	2	y / x		2
1	1.09	1.02	1	1.10	1.02	1	0.6	0.1
2	1.01	0.87	2	1.02	0.84	2	1.1	-3.1
Run 0031-1	8 measure	d void (%)	SIMU	LATE5 voi	d (%)	Di	fferences (/ o)
Cross-secti	onal void	62.30			65.66	Cross-sect	ional void	3.4
Q-assembly	relative voi	elative void		Q-assembly relative void		Q-assembly	d	
y / x	1	2	y / x	1	2	y / x	1	2
1	1.06	1.01	1	1.05	1.01	1	-0.3	0.4
2	1.01	0.92	2	1.02	0.92	2	0.4	0.0
Run 0031-2	1 measure	d void (%)	SIMU	LATE5 voi	d (%)	Di	fferences (%)
Cross-secti	Cross-sectional void		Cross-sectional void		80.33	<u> </u>		2.0
Q-assembly relative void		d	Q-assembly relative void Q-ass			Q-assembly	relative voi	d
y / x	1	2	y / x	1	2	y / x	1	2
1	1.03	1.00	1	1.03	1.01	1	0.5	0.6
2	1.01	0.95	2	1.01	0.95	2	-0.5	-0.7

The main observations from Table 6 and Table 7 are:

- The agreement between the measured and calculated Q-assembly radial void distribution is reasonably good. Differences are in all cases below 5%.
- S5 Q-assembly void distribution is essentially proportional to the 2D relative power density.

• The measured Q-assembly void distribution is flatter than the numerical solution; probably due to S5 assumption that the turbulent mixing and void drift effects are negligible.

4. Conclusions

The two-phase pressure drop results show good agreement with the measurements. The average bias is +1% and the standard deviation 3.6%. The void fraction predictions show good agreement with the measurements. The average bias is +0.2% and the standard deviation 2.3%.

There is good agreement between the S5 predicted mass fluxes in natural and forced circulation and the measured ones at BWR operating pressure. Natural circulation flow at 6.8 MPa is well predicted, except at low heat flux conditions. The mass flow is slightly overestimated at low pump speed and low heat flux conditions.

A partial validation of the quarter-assembly thermal hydraulic model was performed. The S5 model predicts void fractions that are proportional to the Q-assembly power fraction. Thus it over-estimates the void content in the high power quadrant and underestimates the void content in the low power quadrant.

5. References

- [1] T. Bahadir, S-Ö Lindahl, "Studsvik's Next Generation Nodal Code SIMULATE5", ANFM, Hilton Head Island, South Carolina, USA (2009).
- [2] S-Ö Lindahl, T. Bahadir, G. Grandi, "SIMULATE-4 developments", PHYSOR 2008, Interlaken, Switzerland (2008).
- [3] T. Bahadir, S-Ö Lindahl, "Evaluation of Gamma Scanning in Oskarshamn2 With SIMULATE5", PHYSOR 2010, Pittsburgh, Pennsylvania, USA (2010).
- [4] O. Nylund R. Eklund, O. Gelius and G. Manov, "OF-64 General on the experiments", FRIGG PM-55, Asea Atom, August 1969.
- [5] NEA/NRC, "NUPEC BWR Full-size Fine-mesh Bundle Test (BFBT) Benchmark Volume I: Specifications", NEA/NSC/DOC(2005)5, 2006.
- [6] R.T. Lahey Jr. and F.J.Moody, "The Thermal Hydraulic of a Boiling Water Reactor", ANS, (1993).
- [7] G. S. Lellouche, and B. A. Zolotar, "Mechanistic model for predicting two-phase void fraction for water in vertical tubes, channels and rod bundles, EPRI-NP2246-SR, (1982).
- [8] O. Gelius and G. Manov, "OF-64 Results of pressure drop measurements", FRIGG PM-71, Asea Atom, May 1970.
- [9] O. Nylund R. Eklund, "OF-64 Results of void measurements", FRIGG PM-69, Asea Atom, February 1970.

[10] R. Eklund, O. Nylund and A. Jensen, "OF-64 Hydraulic Characteristics and Stability Limits", FRIGG PM-68, Asea Atom, February 1970.

6. Appendix

For the statistical evaluation of the results the average or mean deviation (bias),

$$bias = \frac{1}{n} \sum_{i=1}^{n} \varepsilon_i \tag{1}$$

and the standard deviation (stddev) are used,

$$stddev = \sqrt{\frac{1}{n-1} \sum_{i=1}^{n} (\varepsilon_i - bias)^2}$$
(2)

In Eq. (1) and (2) n is the number of measured points, and ε is the relative error, computed as,

$$\varepsilon_i = \frac{y_i^{calc} - y_i^{meas}}{y_i^{meas}} \tag{3}$$

with y^{calc} and y^{meas} are the calculated and measured quantities respectively.